Report

Geochemical provenancing and direct dating of the Harbin archaic human cranium

Qingfeng Shao,[1,12] Junyi Ge,[2,3,12] Qiang Ji,[4,*] Jinhua Li,[5] Wensheng Wu,[4] Yannan Ji,[6] Tao Zhan,[7] Chi Zhang,[2,3] Qiang Li,[2,3] Rainer Grün,[8,9,*] Chris Stringer,[10,*] and Xijun Ni[2,3,4,11,*]

*Correspondence: nixijun@hgu.edu.cn (X.N.); jiqiang@hgu.edu.cn (Q.J.); rainer.grun@griffith.edu.au (R.G.); c.stringer@nhm.ac.uk (C.S.)

Received: May 10, 2021; Accepted: June 4, 2021; Published Online: June 25, 2021; https://doi.org/10.1016/j.xinn.2021.100131

© 2021 The Author(s). This is an open access article under the CC BY-NC-ND license (http://creativecommons.org/licenses/by-nc-nd/4.0/).

Graphical abstract

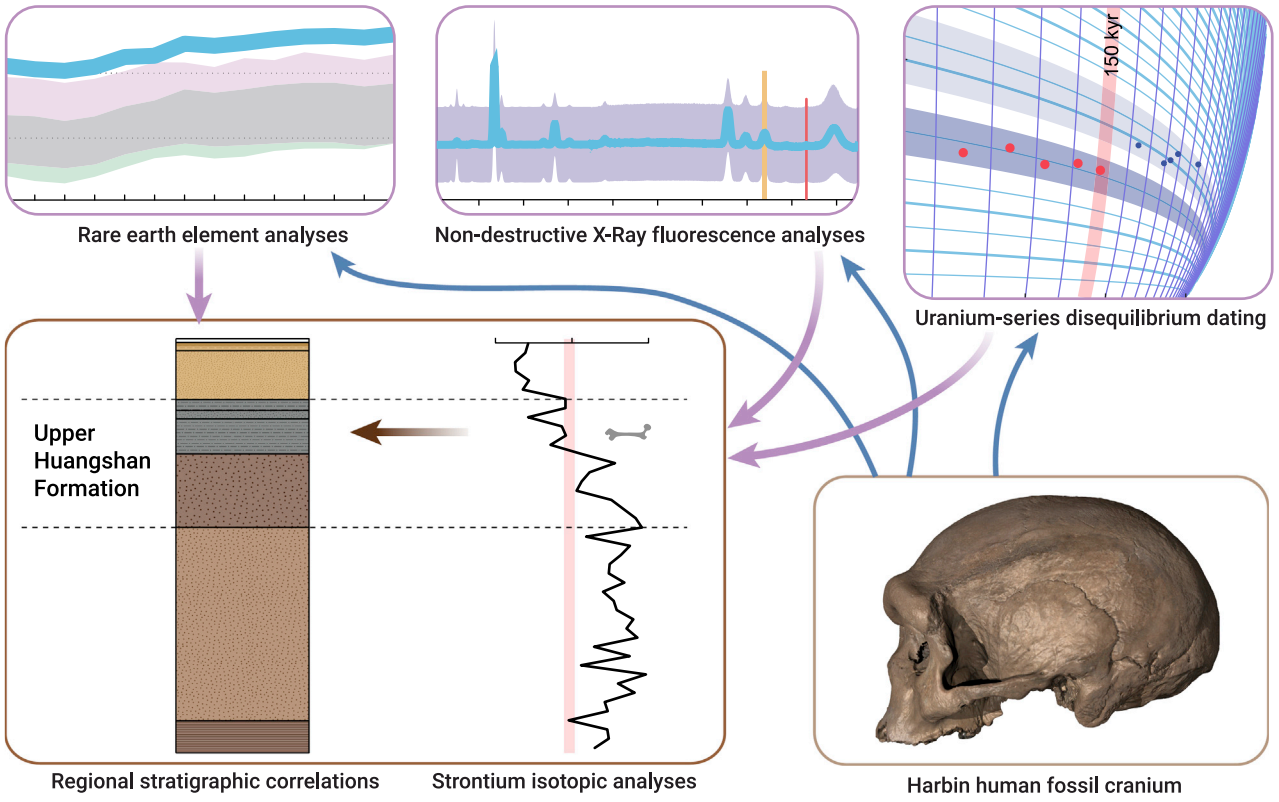

Public summary

- Unsystematic recovery of the Harbin fossil cranium and a long history since the discovery impede its accurate dating
- Geochemical analyses, including non-destructive X-ray fluorescence, rare earth elements, and the strontium isotopes, suggest that the fossil cranium was from a bed of lacustrine sediments aged between 138 and 309 thousand years ago in the Harbin region
- Uranium-series disequilibrium dating directly on the cranium suggests that the cranium is older than 146 thousand years

Report

Geochemical provenancing and direct dating of the Harbin archaic human cranium

Qingfeng Shao,[1,12] Junyi Ge,[2,3,12] Qiang Ji,[4,*] Jinhua Li,[5] Wensheng Wu,[4] Yannan Ji,[6] Tao Zhan,[7] Chi Zhang,[2,3] Qiang Li,[2,3] Rainer Grün,[8,9,*] Chris Stringer,[10,*] and Xijun Ni[2,3,4,11,*]

[1]Key Laboratory of Virtual Geographic Environment, Ministry of Education, Nanjing Normal University, Nanjing 210023, China
[2]CAS Center for Excellence in Life and Paleoenvironment, Chinese Academy of Science, Beijing 100044, China
[3]University of Chinese Academy of Sciences, Beijing 100049, China
[4]Hebei GEO University, Shijiazhuang 050031, China
[5]Key Laboratory of Earth and Planetary Physics, Innovation Academy for Earth Science, Chinese Academy of Sciences, Beijing 100029, China
[6]China Geo-Environmental Monitoring Institute, Beijing 100081, China
[7]The Second Hydrogeology and Engineering Geology Prospecting Institute of Heilongjiang Province, Harbin 150030, China
[8]Australian Research Centre for Human Evolution, Griffith University, Nathan, QLD, Australia
[9]Research School of Earth Sciences, The Australian National University, Canberra, ACT, Australia
[10]Centre for Human Evolution Research, Department of Earth Sciences, Natural History Museum, London, UK
[11]CAS Center for Excellence in Tibetan Plateau Earth Sciences, Chinese Academy of Science, Beijing 100104, China
[12]These authors contributed equally
*Correspondence: nixijun@hgu.edu.cn (X.N.); jiqiang@hgu.edu.cn (Q.J.); rainer.grun@griffith.edu.au (R.G.); c.stringer@nhm.ac.uk (C.S.)
Received: May 10, 2021; Accepted: June 4, 2021; Published Online: June 25, 2021; https://doi.org/10.1016/j.xinn.2021.100131
© 2021 The Author(s). This is an open access article under the CC BY-NC-ND license (http://creativecommons.org/licenses/by-nc-nd/4.0/).
Citation: Shao Q., Ge J., Ji Q., et al., (2021). Geochemical provenancing and direct dating of the Harbin archaic human cranium. The Innovation **2(3)**, 100131.

As one of the most complete archaic human fossils, the Harbin cranium provides critical evidence for studying the diversification of the *Homo* genus and the origin of *Homo sapiens*. However, the unsystematic recovery of this cranium and a long and confused history since the discovery impede its accurate dating. Here, we carried out a series of geochemical analyses, including non-destructive X-ray fluorescence (XRF), rare earth elements (REE), and the Sr isotopes, to test the reported provenance of the Harbin cranium and get better stratigraphic constraints. The results show that the Harbin cranium has very similar XRF element distribution patterns, REE concentration patterns, and Sr isotopic compositions to those of the Middle Pleistocene-Holocene mammalian and human fossils recently recovered from the Harbin area. The sediments adhered in the nasal cavity of the Harbin cranium have a $^{87}Sr/^{86}Sr$ ratio of 0.711898, falling in the variation range measured in a core drilled near the Dongjiang Bridge, where the cranium was discovered during its reconstruction. The regional stratigraphic correlations indicate that the Harbin cranium was probably from the upper part of the Upper Huangshan Formation of the Harbin area, which has an optically stimulated luminescence dating constraint between 138 and 309 ka. U-series disequilibrium dating (n = 10) directly on the cranium suggests that the cranium is older than 146 ka. The multiple lines of evidence from our experiments consistently support the theory that the Harbin cranium is from the late Middle Pleistocene of the Harbin area. Our study also shows that geochemical approaches can provide reliable evidence for locating and dating unsystematically recovered human fossils, and potentially can be applied to other human fossils without clear provenance and stratigraphy records.

Keywords: human fossil provenancing; non-destructive X-ray fluorescence; rare earth elements; strontium (Sr) isotopic composition; uranium-series disequilibrium (U-series) dating

INTRODUCTION

The Middle Pleistocene Harbin human cranium (HBSM2018-000018(A)) is one of the best-preserved of all archaic human fossils, and has great significance for understanding the diversification of the *Homo* genus and the origin of *Homo sapiens*.[1] It represents a new human lineage evolving in East Asia, and is placed as a member of the sister group of *H. sapiens*.[1] A combination of primitive and derived features in the Harbin cranium establishes a good set of diagnostic features that were used to define a new *Homo* species.[2] The Harbin cranium was reportedly discovered in 1933 during construction work when a bridge (Dongjiang Bridge) was built over the Songhua River in Harbin City in Northeastern China[3] (Figure 1). Because of a long, difficult, and confused history since the discovery, the information about the exact geographic origin and stratigraphical context of the cranium has been lost, impeding its accurate dating.[1] Here, we tested the concentrations of rare earth elements (REEs) and the Sr isotopic composition of the human fossil, and a range of mammalian fossils collected from deposits of the Songhua River near the supposed locality (Dongjiang Bridge), and used non-destructive X-ray fluorescence (XRF) analyses to examine the element distributions of these human and mammalian fossils. We also directly dated the Harbin fossil cranium by the uranium-series disequilibrium (U-series) method. The results of these analyses provided consistent evidence for the theory that the Harbin cranium is from the late Middle Pleistocene of the Harbin area.

RESULTS

Non-destructive XRF analyses

The non-destructive XRF analyses were conducted on the Harbin cranium and a range of mammalian fossils collected from the Pleistocene deposits of the Songhua River in Harbin area, Jiangsu Province and Guangxi Province. All the tested samples, including the two control rhinoceros fossils, have a similar XRF pattern in terms of major elements, such as Ca, P, Fe, and Mn, with various concentrations among different samples. The XRF pattern for minor elements, such as Sr, Y, and Zr are obviously different between the tested samples and the control samples (Figure 2A). Zr is undetectable from the two control samples. The Harbin cranium and the mammalian fossils from the Harbin area show almost identical XRF patterns in term of the relative amount of Sr, Y, and Zr (Figure 2A). The XRF analyses support that the Harbin cranium and the collected Harbin mammalian fossils were probably buried and fossilized in the same environment.

REE concentration pattern

The REE concentration pattern has been proved to be an effective tool for tracing the origins of the fossils and living creatures.[7–10] Small bone pieces from the nasal cavity of the Harbin cranium were carefully collected for REE analyses. For comparison, fossil fragments from seven mammals and two human individuals recovered from the deposits of the Songhua River in the Harbin area were also analyzed (Figures S1 and S2). The ages of these

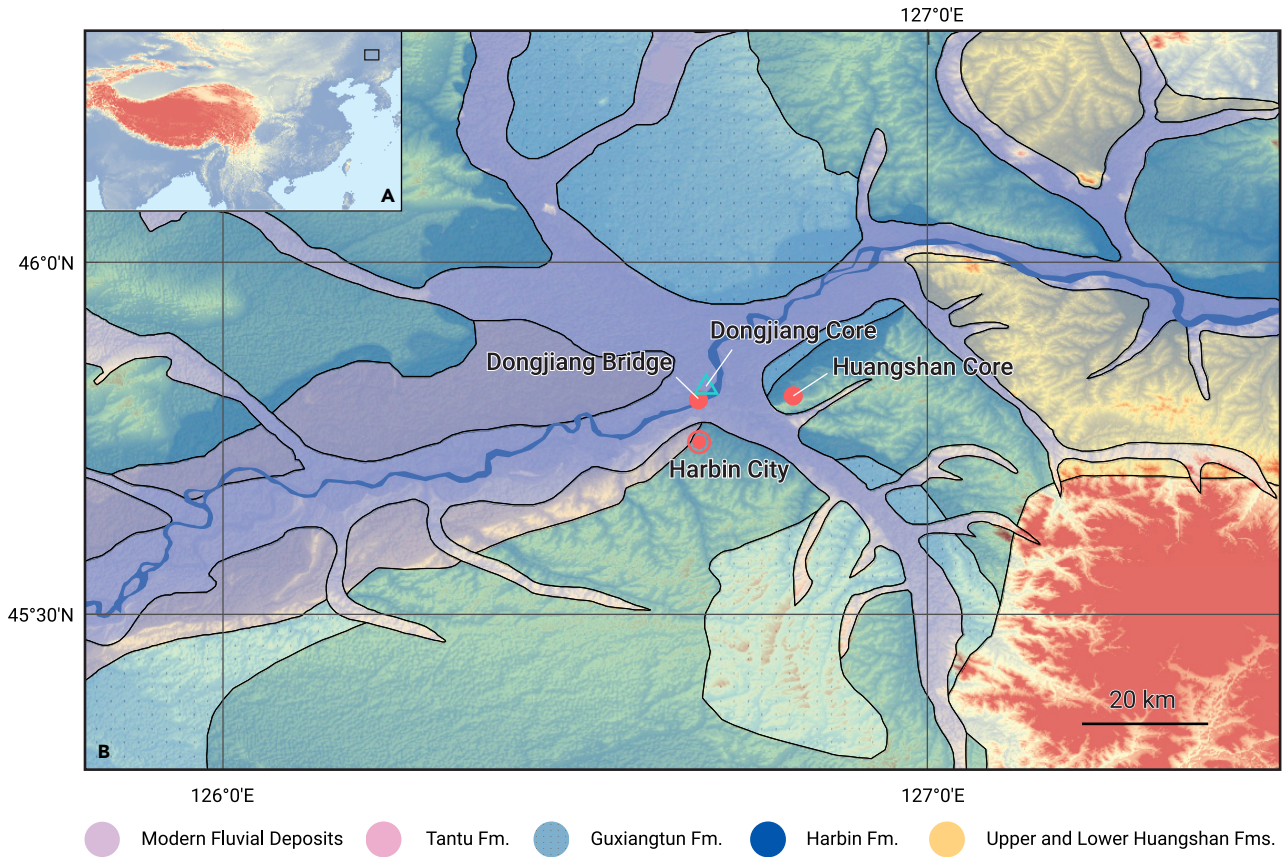

Figure 1. The proposed location of the Harbin fossil cranium (A) DEM image of China, with a rectangle indicating the study area. (B) Geological map of the Harbin area. Revised from the Wang and other workers.[4–6]

comparative specimens range from the Middle Pleistocene to Holocene, as indicated by their U-series apparent ages (Table S1).

The REE concentrations were determined using an HR-ICP-MS (high resolution inductively coupled plasma mass spectrometer). The REE results for the Harbin cranium and those for human/mammalian fossils with a common geographic origin for comparison are listed in Table S1, and shown as REE patterns normalized to PAAS (Post Archean Australian Shale) in a spider diagram in Figure 2B. Both the Harbin cranium and these analyzed fossils exhibit similar REE concentration patterns (Figure 2B). The light REE to heavy REE (LREE/HREE) ratio of the Harbin cranium is 3.668, following the range of these analyzed fossils (3.463–5.514). This range, including that of the Harbin cranium, is much lower than the LREE/HREE of PAAS (9.491), indicating that all these fossils show relatively low fractionation and HREE depletion. The total REE (ΣREE) value of the Harbin cranium is about 234.6 μg/g, higher than those of the fossil specimens analyzed for comparison (with a range from 4.6 to 149.5 μg/g). The high ΣREE value of the Harbin cranium is probably due to its greater age, which results in longer and more complex diagenesis processes. The REE concentration patterns and the LREE/HREE values of the Harbin cranium and the Middle Pleistocene-Holocene human/mammalian fossils suggest that they probably have the same geographical origins.

Strontium isotopic composition

Strontium (Sr) isotopic ratio is widely used as a petrogenetic tracer for determining the source of rock/sediment formations (e.g., Faure[11]). In anthropological and archeological researches, the technique is used to investigate prehistoric human migration,[12–14] ancient animal movements,[15,16] or special events of animal resources use.[17] Sr isotopic analyses were performed on the Harbin cranium (n = 1), and the mammalian fossils (n = 7) and human fossils (n = 2) recovered from the deposits of the Songhua River in the Harbin area, using an MC-ICPMS (multi-collector inductively coupled plasma mass spectrometer, Thermo Fisher Neptune). Moreover, the sediment samples adhering in the nasal cavity of the Harbin cranium (n = 1) and from a core (n = 45) drilled near the Dongjiang Bridge (DJ core, Figure 1B) were also analyzed.

The $^{87}Sr/^{86}Sr$ ratio of the Harbin cranium shows a value of 0.709423 ± 0.000009, comparable with that of the analyzed human/mammalian fossils, ranging from 0.709066 to 0.709574 (Table S2; Figure 3). The Sr isotopic ratios of these fossils all fall in the variation range of the bioavailable Sr in the Harbin areas (0.7070–0.7110, Figure S3). The bioavailable Sr in the Harbin and the nearby areas has the lowest $^{87}Sr/^{86}Sr$ ratios (<0.711) in China (Figure S3), which is thought to be related to the mafic-ultramafic silicate rocks of the Xing'an-Mongolian orogenic belt.[18] These Sr isotopic data strongly suggest that they shared a common geological environment and bioavailable Sr source. The sediments adhered in the nasal cavity of the Harbin cranium consist of dark gray sandstone, most similar to those from the layer between 6.6 and 12.5 m of the DJ core. They yielded a $^{87}Sr/^{86}Sr$ isotopic ratio of 0.711898 ± 0.000003, which falls in the variation ranges measured in the DJ core (from 0.709765 to 0.714884) and is close to the values of the sediments at the depths of ~12 m of the DJ core (Figure 4).

Lithostratigraphic correlation

The sedimentary sequence of the DJ core from the top to the unconformity with the Mesozoic includes nine layers (Figure 4). These layers are correlated with the Huangshan section (Figures 1 and 4), which is a standard section of the regional Quaternary stratigraphy, approximately 15 km from the DJ core.[4] The Huangshan section (HS section) and a core drilled at the Huangshan section (HS core) are well dated by magnetostratigraphic and optically stimulated luminescence (OSL) methods.[4,5] The HS core also has Sr isotopic ratios.[5] The second and third layers from top of the DJ core are

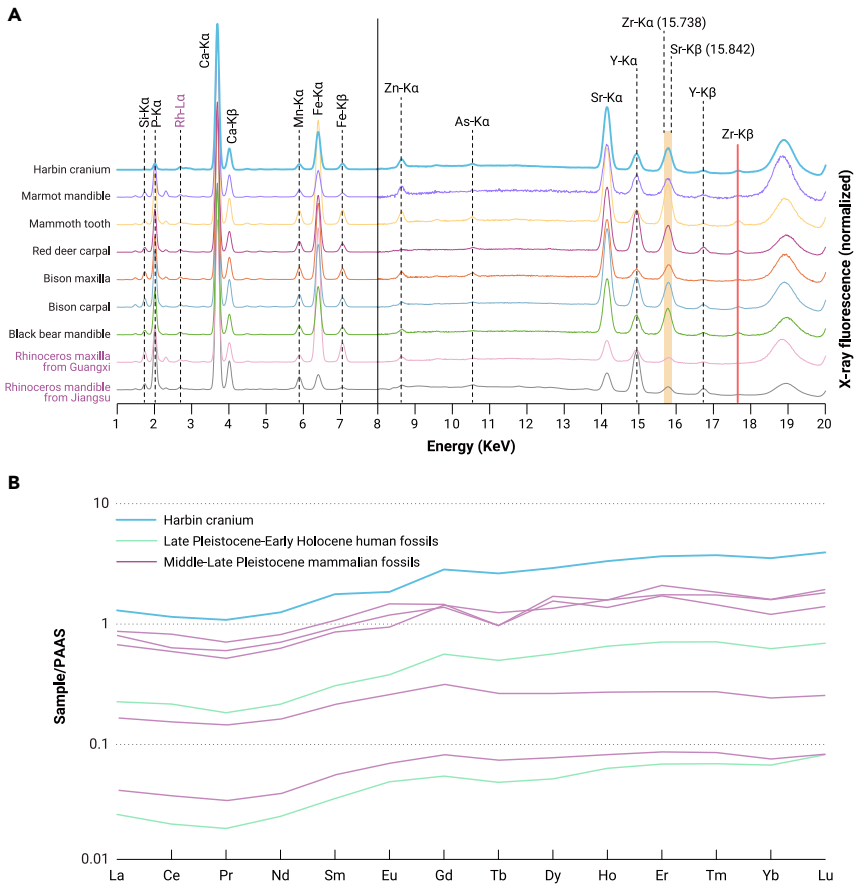

Figure 2. Provenance analyses on the Harbin cranium and the fossil specimens analyzed for comparison (A) XRF element spectra.
(B) REEs. Each XRF spectrum was normalized with the signal of the Rh-Lα peak, which is generated by a Rh X-ray source. The rhinoceros maxilla and mandible from different sites were taken as control samples. The concentration patterns of the REEs were normalized by Post Archean Australian Shale (PAAS).

set of yellowish-brown, alluvial fine muddy silt, alluvial silt, about 6.2 m thick. These two layers can be correlated to the Guxiangtun Formation/Harbin Formation of the HS section/HS core. The fourth to the sixth layers of the DJ core are characterized by gray to dark gray static water deposition of sludge-like mud and alluvial fine silt, about 5.9 m thick. These layers can be roughly correlated with the upper part of the Upper Huangshan Formation of the HS section/HS core, in which there are also more gray to dark gray muddy sediments than in other layers. The seventh and eighth layers of the DJ core include grayish-brown, fluvial sand and alluvial medium-grained sandy silt, about 29 m thick. The two layers should be correlated with the sandier lower part of the Upper Huangshan Formation and the Lower Huangshan Formation of the HS section/HS core.

The Harbin area is one of the most fossiliferous areas in China. More than 70 species have been reported from this area.[19–25] Fossils collected from the deposits in the Songhua River near the Dongjiang Bridge are mainly from the upper yellowish-brown muddy silt layers (~Guxiangtun Formation/Harbin Formation), and the grayish mud and silt (~upper part of the Upper Huangshan Formation). The U-series dating on the fossil samples from seven mammals and two human individuals (Figures S1 and S2) yielded two groups of apparent

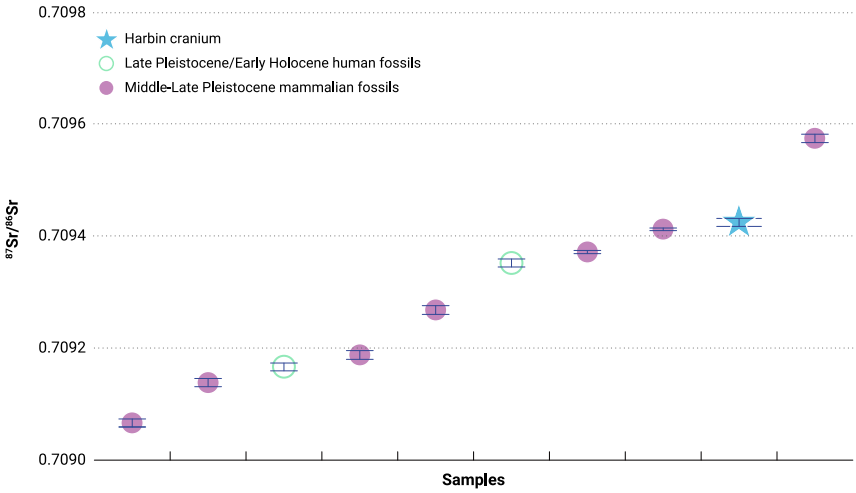

Figure 3. Sr isotopic composition on the Harbin cranium and the Middle Pleistocene-Early Holocene mammalian and human fossils

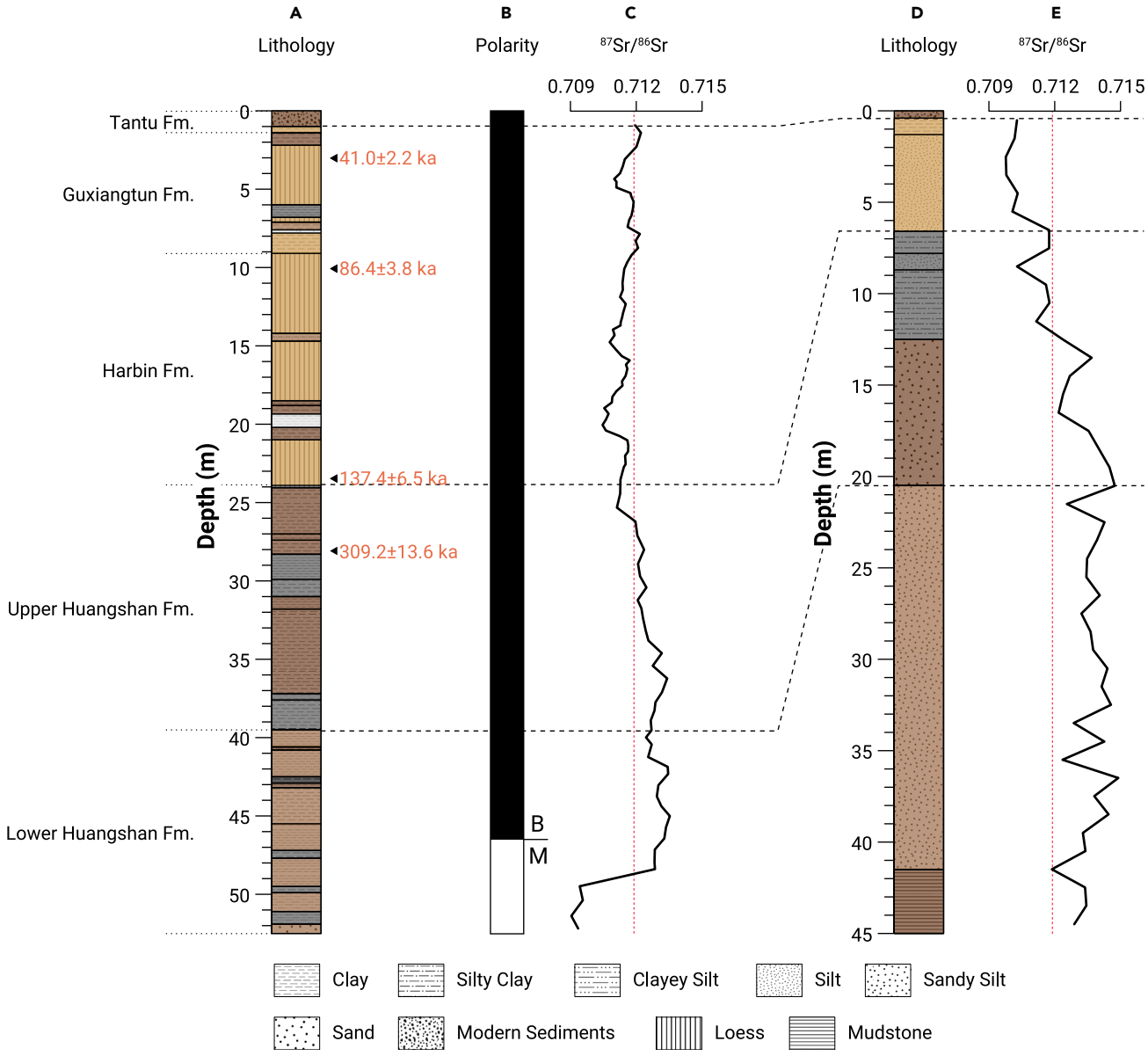

Figure 4. Stratigraphic correlations and the Sr isotopic ratios of the sediments from the Huangshan section, Huangshan core, and Dongjiang core (A and B) Lithostratigraphy and Paleomagnetic polarities from the Huangshan section, based on the data from Wang et al.[4] (C) Sr isotopic ratios from the Huangshan core, data from Wei et al.[5] (D and E) Lithostratigraphy and Sr isotopic ratios from the Dongjiang core, data are from this research. The Dongjiang Bridge core was drilled at 45°50′28″N, 126°36′27″E. The sedimentary sequence of the Dongjiang core from the top to the unconformity with the Mesozoic includes nine layers: (1) modern sediments, 0.4 m; (2) yellowish-brown, alluvial fine muddy silt, 0.9 m; (3) yellowish-brown alluvial silt, 5.3 m; (4) gray to dark gray, static water deposition, sludge-like mud, 1.2 m; (5) dark gray alluvial fine silt, 0.9 m; (6) dark gray, static water deposition, sludge-like mud, 3.8 m; (7) grayish-brown, fluvial sand, including ~3% of gravels, gravel diameter ~3 mm, 8 m; (8) grayish-brown alluvial medium grained sandy silt, 21 m; and (9) grayish-brown, mudstone, with parallel bedding, 3.5 m. The unconformity is between layer 8 and layer 9. The age in red is the OSL date. The red dashed lines indicate the Sr isotope ratio of the sediments adhering in the Harbin cranium.

ages, ranging from 9 ± 4 to 34.6 ± 0.3 ka, and from 132.6 ± 0.4 to 201 ± 1 ka (Table S3). The age of the Guxiangtun Formation/Harbin Formation is known as ~12–138 ka old, and the upper part of the Upper Huangshan Formation has an OSL dating constraints between 138 and 309 ka.[4] The two groups of direct U-series apparent ages of the mammalian/human fossils from the Harbin area fall in the age range of the two formations and are consistent with the stratigraphic correlations.

When the Sr isotopic ratios from the HS core[5] are compared with the DJ core (Figure 4), the fourth to sixth layers between 6.6 and 12.5 m of the DJ core show a similar gradual increase as the upper part of the Upper Huangshan Formation of the HS core at depths of ~30 m, which also yielded Sr isotopic ratios around 0.711898 (Figure 4). This result is also consistent with the stratigraphic correlations.

U-series dating

Owing to the poor provenance, we attempted to directly date this fossil cranium using a U-series method. Fossil bones are less desirable than carbonates for U-series dating, because fossil bones readily take up uranium from groundwater after deposition. However, if the incorporated uranium has not been leached out at some time after bone deposition, the U-series apparent age can provide the minimum age of the fossil.[26]

To minimize destruction on the Harbin fossil cranium, the samples (n = 10) for U-series dating were hand drilled on the broken surfaces of the bones with 0.3 mm carbide-tipped drill bits, and the powdered sample size was kept between 0.1 and 0.5 mg (Figure 5). The U and Th isotopic measurements were performed on an MC-ICPMS (Thermo Fisher Neptune). The U-series dating results are summarized in Table S3. All samples lie within a narrow $^{234}U/^{238}U$ activity ratio range (1.481–1.576), but show large variations in

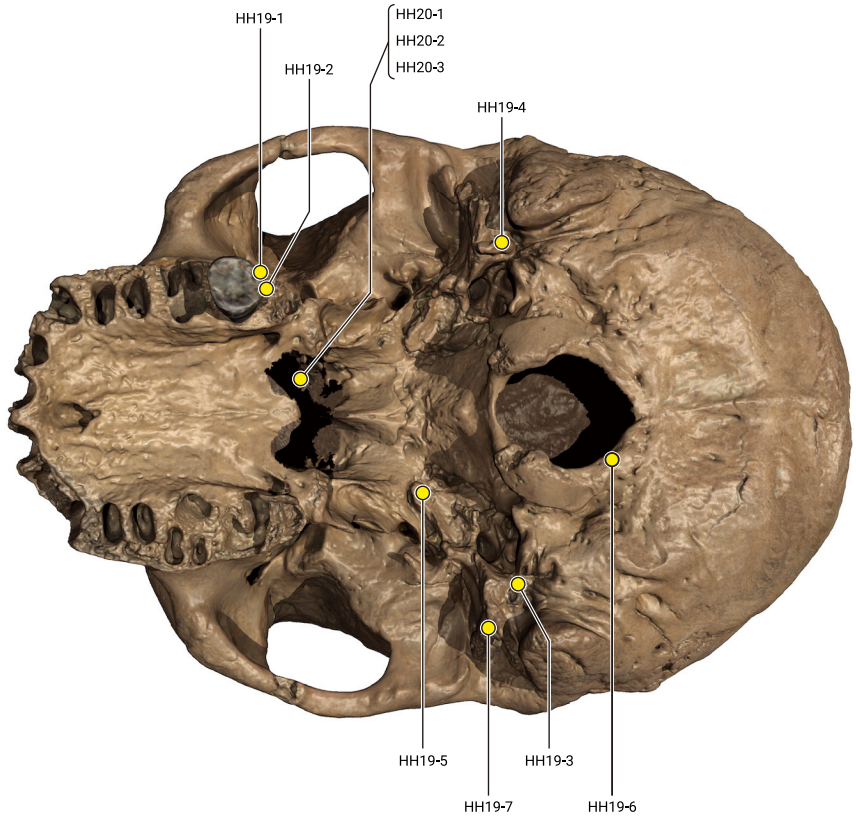

Figure 5. Sampling locations on the Harbin cranium for U-series dating analyses

$^{230}Th/^{234}U$ activity ratio (0.474–1.039). The corrected U-series apparent ages are highly scattered, ranging from 62 ± 3 to 296 ± 8 ka, and the back-calculated initial $^{234}U/^{238}U$ activity ratio ($^{234}U/^{238}U_i$) ranged from 1.652 to 2.161 (Table S3).

The results can roughly be divided into two groups. The first group includes five samples that have relatively younger U-series apparent ages (from 62 ± 3 to 148 ± 2 ka), red data points in the isotope evolution diagram (Figure 6). Their isotopic data randomly scatter around the U-series evolution curve for an initial $^{234}U/^{238}U_i$ of 1.70 (Figure 6). This pattern suggests that the source of uranium in these samples remained the same, but U-uptake took place over different time intervals without obvious evidence for post-burial U-leaching. The two youngest U-series apparent ages are 62 ± 3 and 85 ± 4 ka (HH19-1, 2), both obtained on the exposed dentine from the tooth roots of the surviving molar (M^2). The young ages are probably caused by a delayed U-uptake, because the cementum and dentine of the tooth roots are much denser than the bones and probably obstructed uranium migration into the dentine. The other three U-series apparent ages, 106 ± 1, 129 ± 1, and 148 ± 2 ka, were obtained on HH19-6, 20-2, and 19-4, respectively. This group of data has no obvious evidence for U-leaching and is reasonable for estimating the minimum age of the Harbin cranium. The best minimum age estimate derived from this data group is the maximum value of the data group: that is 148 ± 2 ka.

The second group (green data points in Figure 6) includes five samples with relatively older U-series apparent ages (185 ± 2 to 296 ± 8 ka). This older age group shows higher $^{230}Th/^{234}U$ isotope ratios and more widely scattered initial $^{234}U/^{238}U_i$ ratios than the younger age group. It can be expected that, for a bone that experienced continuous U-uptake process, its $^{230}Th/^{234}U$ activity ratio should be less than 1, but the occurrence of U-leaching can result in a shift of the $^{230}Th/^{234}U$ activity ratio to higher values, even beyond isotopic equilibrium.[27] The subsample HH19-3 shows the oldest apparent U-series age of ~296 ka, but it has ^{230}Th activities in excess of ^{234}U ($^{230}Th/^{234}U$ = 1.031 ± 0.006), suggesting that this old age is very likely the result of U-leaching. The other four subsamples with older ages (HH19-5, 19-7, 20-1, and 20-3) have $^{230}Th/^{234}U$ ratios close to isotopic equilibrium (0.943 on average), suggesting that a slight U-leaching has occurred to these samples. Leached samples do not provide any useful age information, we therefore regard the age of 146 ka from the younger age group as the most conservative age (minimum age) estimate for the Harbin cranium.

The U-series apparent ages of the mammalian/human fossils from the Harbin area (Figures S1 and S2; Table S3) can be seen as the minimum ages of the corresponding fossil samples, except for the samples V23288 and F12, because their ^{230}Th activities are in excess of ^{234}U, and thus the occurrence of U-leaching cannot be excluded. All these samples show initial $^{234}U/^{238}U_i$ (1.467–2.063) comparable with the values measured in the Harbin cranium (1.652–2.161), which provide another line of evidence that the Harbin cranium was probably from a similar burial environment as these fossils analyzed for comparison.

DISCUSSION AND CONCLUSIONS

Our analyses reveal that the Harbin cranium has XRF element distribution patterns and REE concentration patterns like those of the mammalian and human fossils recovered from the Pleistocene sediments in the Harbin area. The $^{87}Sr/^{86}Sr$ ratio of the Harbin cranium (0.709423) also falls in the range of these mammalian and human fossils for comparison (ranging from 0.709066 to 0.709574). All these $^{87}Sr/^{86}Sr$ ratios are within the range of the regional bioavailable Sr isotope ratio values in the Harbin areas. The sediments adhered in the nasal cavity of the Harbin cranium show a $^{87}Sr/^{86}Sr$ ratio of 0.711898, very close to the values measured at the upper part of the DJ core at a depth of ~12 m. The regional stratigraphic correlations based on Sr isotopic data and lithostratigraphic characters indicate that the Harbin cranium probably was recovered from the upper part of the Upper Huangshan Formation. Direct U-series dating on the cranium (n = 10) suggests that one group of the samples suffered U-leaching, and one group of the samples experienced continuous or delayed U-uptake without obvious evidence of U-leaching. The group without U-leaching yielded an apparent age of ~146 ka as the most conservative age (minimum age) estimate for the Harbin cranium. This minimum age is consistent with the regional stratigraphic correlation. While the multiple lines of evidence from

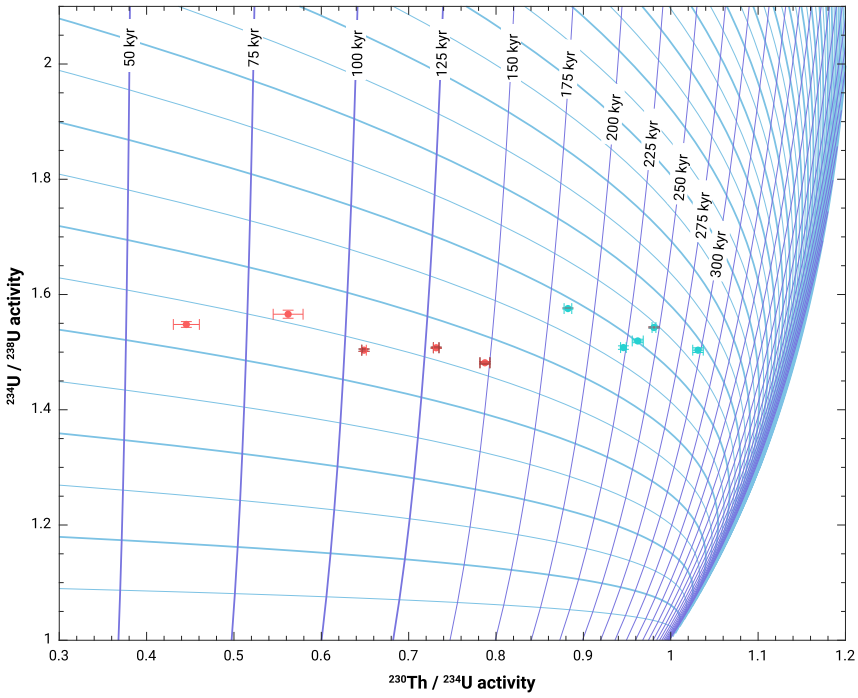

Figure 6. U-series evolution diagram showing the activity ratios observed on the Harbin cranium Light blue lines show U-series evolution in closed-system for selected initial $^{234}U/^{238}U$ values. Red data points randomly scattered around the evolution curve with initial $^{234}U/^{238}U$ of 1.70 are considered to be the results of U-uptake processes without the effect of U-leaching. Green data points are probably the results of U-uptake followed by U-leaching.

our experiments cannot pin the Harbin cranium to an exact site and layer, they consistently support the conclusion that this human specimen is from the late Middle Pleistocene of the Harbin area.

The late Middle Pleistocene Harbin archaic human (>146 ka) is roughly contemporaneous with some other Middle Pleistocene archaic humans from China, such as Xiahe (≥160 ka),[28] Jinniushan (≥200 ka),[29] Dali (327–240 ka),[30,31] and Hualongdong (345–265 ka).[32] This age span also overlaps with the early *H. sapiens* from Africa and the Mideast. If these East Asian archaic humans indeed belong to a monophyletic evolutionary lineage sister to the *H. sapiens* lineage,[1] this human lineage must have been as successful as the early *H. sapiens* populations in Africa and the Mideast, because they distributed in a very large area, including some extreme environments (high altitude and high latitude).

MATERIAL AND METHODS

Provenance test

We used non-destructive XRF analyses, following the procedures of Li et al.,[33] to examine the element distribution of the Harbin cranium and a range of mammalian fossils (n = 6) collected from submerged sediments near the Dongjiang Bridge (Figure 1). The mammalian fossils are Middle-Late Pleistocene in age. Two mammalian fossils from sites in southern China were used as control samples. All the fossil specimens are under the oversight of the institutional review board of the Hebei GEO University or the Institute of Vertebrate Paleontology and Paleoanthropology. XRF analyses were performed on the M4 TORADO PLUS Micro-SRF analyzer at the Institute of Geology and Geophysics, Chinese Academy of Sciences. One area of about ~1–2 cm^2 for each sample was randomly selected for collecting the XRF signals. Measuring parameters were set at 50 kV of high voltage and 40 μm of pixel size. For semi-quantitative comparisons, each XRF spectrum was normalized with the signal of the Rh-Lα peak, which is generated by a Rh X-ray source.

Small bone pieces (~100 mg) from the nasal cavity of the Harbin cranium were carefully collected for REE and Sr isotopic analyses. For comparison, fossil fragments from mammals (Figure S1, n = 6) and late Pleistocene-Holocene human individuals (Figures S2 and S3, n = 2) recovered from the Dongjiang Bridge area were analyzed. The sediment samples adhering in the nasal cavity of the Harbin cranium (n = 1) and from a core (n = 45) drilled near the Dongjiang Bridge were also used for Sr isotopic analyses.

REE analyses were performed at the State Key Laboratory for Mineral Deposits Research, Nanjing University. A Thermo Fisher Element XR HR-ICP-MS was used for the REE analyses. The samples were processed using the method in Trueman et al.[34] The rhodium solution (10 ppb) was dropped into the sample solutions for instrument drift correction. Analytical precision was <5% for each element. An MC-ICPMS (multiple collector inductively coupled plasma mass spectrometer, Thermo Fisher Neptune) in Nanjing Normal University was used for the Sr isotopic analyses. Sample preparation and measurement methods followed that of Lei et al.[35] The measured $^{87}Sr/^{86}Sr$ ratio was corrected for mass fractionation by normalization to a constant $^{86}Sr/^{88}Sr$ ratio of 0.1194 using an exponential law. The isobaric interference of ^{87}Rb on ^{87}Sr was corrected using a natural $^{87}Rb/^{85}Rb$ ratio of 0.3857. Replicate measurements of the NIST SRM 987 standard yielded a mean value of $^{87}Sr/^{86}Sr$ = 0.710263 ± 0.000014 (2σ, n = 11) during the analytical period.

U-series analysis

We carried out the U-series analysis directly on the Harbin cranium. Sample preparation followed that of Shao et al.[36] The U and Th isotopic measurements were performed on an MC-ICPMS (Thermo Fisher Neptune) in Nanjing Normal University. It is equipped with nine Faraday cups and a secondary electron multiplier (SEM). A retarding potential quadrupole energy filter was positioned in front of the SEM. An Aridus-II desolvator system (Cetac) couple with an ESI-50 nebulizer and an AutoSampler (ASX-520) was used for sample introduction. The U-series analysis results are summarized in Table S3. The isotopic variation and age distribution indicate that the U-uptake histories are heterogeneous in the Harbin cranium. A group of samples showing no evidence of U-leaching[26] had a U-series apparent age range of 62 ± 3 to 148 ± 2 ka. We consider that the oldest U-series apparent age (148 ± 2 ka) is a minimum age estimate for the Harbin cranium.

REFERENCES

1. Ni, X., Ji, Q., Wu, W., et al. (2021). Massive cranium from Harbin establishes a new Middle Pleistocene human lineage in China. The Innovation ***2***, 100130. In this issue. https://doi.org/10.1016/j.xinn.2021.100130.
2. Ji, Q., Wu, W., Ji, Y., et al. (2021). Late Middle Pleistocene Harbin cranium represent a new *Homo* species. The Innovation ***2***, 100132. In this issue. https://doi.org/10.1016/j.xinn.2021.100132.
3. Ji, Q., Ji, Y., Wang, X., et al. (2018). Discovery of *Homo heidelbergensis*-like skull fossil in Northeast China. J. Geol. ***42***, 349–350.
4. Wang, Y., Dong, J., and Yang, J. (2020). Quaternary stratigraphy of the Huangshan section in Harbin. Ear. Sci. ***45***, 2662–2672.
5. Wei, Z., Xie, Y., Kang, C., et al. (2020). The inversion of the Songhua River system in the early Pleistocene: implications from Sr-Nd isotopic composition in the Harbin Huangshan cores. Act. Sedimentol. Sin. ***38***, 1192–1203. https://doi.org/10.14027/j.issn.1000-0550.2019.112.
6. Bureau of Geology and Mineral Resources of Heilongjiang Province (BGMRHP). (1993). Regional Geology of Heilongjiang Province. People's Republic of China, Ministry of Geology and Mineral Resources (Geological Memoirs (Geological Publishing House), p. 734.

7. Grandstaff, D.E., and Terry, D.O. (2009). Rare earth element composition of Paleogene vertebrate fossils from Toadstool Geologic Park, Nebraska, USA. Appl. Geochem. ***24***, 733–745. https://doi.org/10.1016/j.apgeochem.2008.12.027.
8. Dalton, R. (2009). Elements reveal fossils' origins. Nature ***459***, 309. https://doi.org/10.1038/459307a.
9. Suarez, C.A., Macpherson, G.L., González, L.A., et al. (2010). Heterogeneous rare earth element (REE) patterns and concentrations in a fossil bone: implications for the use of REE in vertebrate taphonomy and fossilization history. Geochim. Cosmochim. Act. ***74***, 2970–2988. https://doi.org/10.1016/j.gca.2010.02.023.
10. Herwartz, D., Tütken, T., Jochum, K.P., et al. (2013). Rare earth element systematics of fossil bone revealed by LA-ICPMS analysis. Geochim. Cosmochim. Act. ***103***, 161–183. https://doi.org/10.1016/j.gca.2012.10.038.
11. Faure, G. (1977). Principles of Isotope Geology (John Wiley and Sons, Inc.), p. 464.
12. Richards, M., Harvati, K., Grimes, V., et al. (2008). Strontium isotope evidence of Neanderthal mobility at the site of Lakonis, Greece using laser-ablation PIMMS. J. Archaeol. Sci. ***35***, 1251–1256. https://doi.org/10.1016/j.jas.2007.08.018.
13. Copeland, S.R., Sponheimer, M., de Ruiter, D.J., et al. (2011). Strontium isotope evidence for landscape use by early hominins. Nature ***474***, 76–78. https://doi.org/10.1038/nature10149.
14. Lugli, F., Cipriani, A., Capecchi, G., et al. (2019). Strontium and stable isotope evidence of human mobility strategies across the Last Glacial Maximum in southern Italy. Nat. Ecol. Evol. ***3***, 905–911. https://doi.org/10.1038/s41559-019-0900-8.
15. Balasse, M., Smith, A.B., Ambrose, S.H., et al. (2003). Determining sheep birth seasonality by analysis of tooth enamel oxygen isotope ratios: the Late Stone Age site of Kasteelberg (South Africa). J. Archaeol. Sci. ***30***, 205–215. https://doi.org/10.1006/jasc.2002.0833.
16. Britton, K., Grimes, V., Niven, L., et al. (2011). Strontium isotope evidence for migration in late Pleistocene Rangifer: implications for Neanderthal hunting strategies at the Middle Palaeolithic site of Jonzac, France. J. Hum. Evol. ***61***, 176–185. https://doi.org/10.1016/j.jhevol.2011.03.004.
17. Madgwick, R., Lamb, A.L., Sloane, H., et al. (2019). Multi-isotope analysis reveals that feasts in the Stonehenge environs and across Wessex drew people and animals from throughout Britain. Sci. Adv. ***5***, eaau6078. https://doi.org/10.1126/sciadv.aau6078.
18. Wang, X., and Tang, Z. (2020). The first large-scale bioavailable Sr isotope map of China and its implication for provenance studies. Earth Sci. Rev. ***210***, 103353. https://doi.org/10.1016/j.earscirev.2020.103353.
19. Institute of Vertebrate Paleontology CAS. (1959). Pleistocene Mammalian Fossils from the Northeastern Provinces (Science Press), p. 82.
20. Zhengyi, W. (1973). The Quaternary mammalian fossils discovered in the Heilongjiang Province. Chin. Sci. Bull. ***18***, 38–40.
21. Cai, B., and Yin, J. (1992). Late Pleistocene fossil mammals from Qinggang, Heilongjiang Province. Bull. Chin. Acad. Geolog. Sci. ***25***, 131–138.
22. Huili, Y., and Wei, D. (2011). Pleistocene mammalian fauna from the Jiaojie Cave at Acheng, Heilongjiang Province. Quat. Sci. ***31***, 675–688.
23. Yang, Y., Li, Q., Fostowicz-Frelik, Ł., et al. (2019). Last record of *Trogontherium cuvieri* (Mammalia, Rodentia) from the late Pleistocene of China. Quat. Int. ***513***, 30–36. https://doi.org/10.1016/j.quaint.2019.01.025.
24. Ni, X., Li, Q., Stidham, T.A., et al. (2020). Earliest-known intentionally deformed human cranium from Asia. Archaeol. Anthropol. Sci. ***12***, 93. https://doi.org/10.1007/s12520-020-01045-x.
25. Lu, D., Yang, Y., Li, Q., et al. (2020). A late Pleistocene fossil from Northeastern China is the first record of the dire wolf (Carnivora: *Canis dirus*) in Eurasia. Quat. Int. ***591***, 87–92. https://doi.org/10.1016/j.quaint.2020.09.054.
26. Grün, R., Eggins, S., Kinsley, L., et al. (2014). Laser ablation U-series analysis of fossil bones and teeth. Palaeogeogr. Palaeoclimatol. Palaeoecol. ***416***, 150–167. https://doi.org/10.1016/j.palaeo.2014.07.023.
27. Duval, M., Aubert, M., Hellstrom, J., et al. (2011). High resolution LA-ICP-MS mapping of U and Th isotopes in an early Pleistocene equid tooth from Fuente Nueva-3 (Orce, Andalusia, Spain). Quat. Geochronol. ***6***, 458–467. https://doi.org/10.1016/j.quageo.2011.04.002.
28. Chen, F., Welker, F., Shen, C.-C., et al. (2019). A late Middle Pleistocene Denisovan mandible from the Tibetan plateau. Nature ***569***, 409–412. https://doi.org/10.1038/s41586-019-1139-x.
29. Lu, Z., Meldrum, D.J., Huang, Y., et al. (2011). The Jinniushan hominin pedal skeleton from the late Middle Pleistocene of China. Homo ***62***, 389–401. https://doi.org/10.1016/j.jchb.2011.08.008.
30. Wu, X. (2020). Middle Pleistocene human skull from Dali, China. Palaeont. Sin. N. Ser. D ***13***, 1–205.
31. Wu, X., and Athreya, S. (2013). A description of the geological context, discrete traits, and linear morphometrics of the Middle Pleistocene hominin from Dali, Shaanxi Province, China. Am. J. Phys. Anthropol. ***150***, 141–157.
32. Wu, X.-J., Pei, S.-W., and Cai, Y.-J. (2019). Archaic human remains from Hualongdong, China, and Middle Pleistocene human continuity and variation. Proc. Natl. Acad. Sci. U S A ***116***, 9820–9824. https://doi.org/10.1073/pnas.1902396116.
33. Li, J., Pei, R., Teng, F., et al. (2021). Micro-XRF study of the troodontid dinosaur Jianianhualong tengi reveals new biological and taphonomical signals. Atom. Spectrosc. ***42***, 1–11.
34. Trueman, C.N., Behrensmeyer, A.K., Potts, R., et al. (2006). High-resolution records of location and stratigraphic provenance from the rare earth element composition of fossil bones. Geochim. Cosmochim. Act. ***70***, 4343–4355. https://doi.org/10.1016/j.gca.2006.06.1556.
35. Lei, H.-L., Yang, T., Jiang, S.-Y., et al. (2019). A simple two-stage column chromatographic separation scheme for strontium, lead, neodymium and hafnium isotope analyses in geological samples by thermal ionization mass spectrometry or multi-collector inductively coupled plasma mass spectrometry. J. Sep. Sci. ***42***, 3261–3275. https://doi.org/10.1002/jssc.201900579.
36. Shao, Q.-F., Li, C.-H., Huang, M.-J., et al. (2019). Interactive programs of MC-ICPMS data processing for 230Th/U geochronology. Quat. Geochronol. ***51***, 43–52. https://doi.org/10.1016/j.quageo.2019.01.004.

ACKNOWLEDGMENTS

We thank colleagues of the Heilongjiang Academy of Geological Sciences who helped with core drilling and sample collections. Drs. T. Yang and H.-L. Lei from the Nanjing University helped with the REE and Sr isotopic analyses. Dr. Z. Tang provided the recent published bioavailable Sr isotopic mapping data. We are grateful for the support of Drs. F. Wang, C. Li, X. Wu, D. Zhang, L. Crété, and T. Deng, as well as R. Tang for his help on making the figures. We thank Dr. Y.-Y. Xie from the Harbin Normal University for providing the Sr isotope ratio data of the Huangshan core. This project has been supported by the National Natural Science Foundation of China (41977380, 41877430, 41842039, 41625005, 41888101, 41988101), the Strategic Priority Research Program of Chinese Academy of Sciences (CAS XDB26030400, XDB26030300, XDA20070203, XDA19050100), the People's Government of Hebei Province (Z20177187), the China Geological Survey (DD20190601), the Science Foundation of Hebei GEO University (TS2017-001), and the Second Tibetan Plateau Scientific Expedition and Research Program (2019QZKK0705). C.S.'s research is supported by the Calleva Foundation and the Human Origins Research Fund. We thank the reviewers for their help in improving the article.

AUTHOR CONTRIBUTIONS

Q.J. obtained the Harbin cranium and organized the project. Q.S. performed U-series dating, REE and Sr isotopic analyses, analyzed the U-series dating data, and wrote the manuscript. J.G. analyzed the REE and Sr isotopic data, and wrote the manuscript. J.L. performed XRF analyses, and edited the manuscript. R.G. analyzed the U-series dating data, and edited the manuscript. Q.L. collected the mammalian fossils, and edited the manuscript. W.W., Y.J., and T.Z. collected data, drilled the core, and measured sections. C.S. and C.Z. edited the manuscript. X.N. analyzed the data, organized the project, and wrote the manuscript.

DECLARATION OF INTERESTS

The authors declare no competing interests.

SUPPLEMENTAL INFORMATION

Supplemental information can be found online at https://doi.org/10.1016/j.xinn.2021.100131.

The Innovation, Volume *2*

Supplemental Information

Geochemical provenancing and direct dating of the Harbin archaic human cranium

Qingfeng Shao, Junyi Ge, Qiang Ji, Jinhua Li, Wensheng Wu, Yannan Ji, Tao Zhan, Chi Zhang, Qiang Li, Rainer Grün, Chris Stringer, and Xijun Ni

SUPPLEMENTAL INFORMATION

Title:

Geochemical provenancing and direct dating of the Harbin archaic human cranium

Authors list:

Qingfeng Shao[1,12], Junyi Ge[2, 3,12], Qiang Ji[4*], Jinhua Li[5], Wensheng Wu[4], Yannan Ji[6], Tao Zhan[7], Chi Zhang[2, 3], Qiang Li[2, 3], Rainer Grün[8,9*], Chris Stringer[10*], Xijun Ni[2, 3, 4, 11*]

Affiliations:

1. Key Laboratory of Virtual Geographic Environment, Ministry of Education, Nanjing Normal University, Nanjing, 210023, China
2. CAS Center for Excellence in Life and Paleoenvironment, Chinese Academy of Science, Beijing, 100044, China
3. University of Chinese Academy of Sciences, Beijing, 100049, China
4. Hebei GEO University, Shijiazhuang, Hebei Province, 050031, China
5. Key Laboratory of Earth and Planetary Physics, Innovation Academy for Earth Science, Chinese Academy of Sciences, Beijing 100029, China
6. China Geo-Environmental Monitoring Institute, Beijing, 100081, China
7. The Second Hydrogeology and Engineering Geology Prospecting Institute of Heilongjiang Province, Harbin 150030, China
8. Australian Research Centre for Human Evolution, Griffith University, Nathan, Queensland, Australia
9. Research School of Earth Sciences, The Australian National University, Canberra, ACT, Australia
10. Centre for Human Evolution Research, Department of Earth Sciences, Natural History Museum, London, UK
11. CAS Center for Excellence in Tibetan Plateau Earth Sciences, Chinese Academy of Science, Beijing, 100104, China
12. Co-first authors

Correspondence:

* nixijun@hgu.edu.cn (X.N.); jiqiang@hgu.edu.cn (Q.J.); rainer.grun@griffith.edu.au (R.G.); c.stringer@nhm.ac.uk (C.S.)

Regional Stratigraphy

The Quaternary lithostratigraphy in the Harbin region include 5 units from the top to the bottom[1-3]: Tantu Formation, Guxiangtun Formation, Harbin Formation, Upper Huangshan Formation and Lower Huangshan Formation (Fig. 1). The uppermost Tantu Formation spreads on the floodplain of Songhua River mainly west to the Harbin city. The formation consists of a series of Holocene dark brown, grayish brown and grayish black alluvial- fluvial clay and sandy clay. The Guxiangtun Formation consists of yellowish brown, grayish brown, and grayish black silty clay, loess and sandstone of fluvial-lacustrine origin. The formation is widely distributed on the lower terraces or higher floodplains of the Songhua River. The upper part of the Guxiangtun Formation includes mainly dark brown or grayish black clay, and yellowish brown loess with bends of palaeosoil. The lower part of the Guxiangtun Formation includes reworked loess, dark brown and grayish black sandy clay, silt and clay. There are a large amount of charcoal grains in the lower part of the formation. The age of this formation is between ~12 ka and ~79 ka[2]. The Harbin Formation consists of mainly yellowish-brown and yellow aeolian loess with bends of paleosoils. The formation is partially exposed on the lower terrace of the Songhua River and parts of the floodplain in the Harbin region. The formation was recently dated between ~138 ka and ~79 ka[2]. The Upper Huangshan Formation is characterized by greenish-gray, grayish-brown, and dark gray muddy siltstone or silty mudstone with a few lenticular fine sandstone layers of fluvial-lacustrine origins. The age of the Upper Huangshan Formation is between ~580 ka and ~138 ka[2]. This formation is mainly distributed on the higher terrace or on the piedmonts in the east and northeast areas of Songhua River floodplain. The Upper Huangshan Formation overlays the Lower Huangshan Formation. The upper part of the Lower Huangshan Formation mainly consists of brownish-gray to dark gray lacustrine sandy mudstone. The lower part of the Lower Huangshan Formation is a set of grayish-brown or yellowish-brown fluvial sandstone. The Lower Huangshan Formation is scarcely exposed at a few thick sediment sections[2, 4]. The uppermost Lower Huangshan Formation is currently dated as ~580 ka[2]. The bottom of the Lower Huangshan Formation is not exposed. It is believed that the whole formation belongs to the late Early Pleistocene and early Middle Pleistocene[2, 4].

The five formations are all fossiliferous. The whole area is indeed one of the most fossiliferous areas in China. Mammalian fossils from the Guxiangtun Formation and the Upper Huangshan Formation are extremely common. Thousands of mammalian fossils and many human fossils were collected from the underwater sand mine sites in the Songhua River near the Harbin City. Because the mining activities are well monitored and controlled, it is clear now that these fossils are mainly collected from the sediments of the Guxiangtun Formation and the upper part of the Upper Huangshan Formation of these underwater sand mine sites. More than 70 species have been reported from the area[5-11].

X-Ray fluorescence (XRF) analyses.

XRF analyses were performed on the M4 TORADO PLUS Micro-SRF analyzer at the Institute of Geology and Geophysics, Chinese Academy of Sciences, following the procedures of Li et al. [12]. In order to avoid system error caused by the measurement setting and the unevenness

of the test region, one area of about ~1-2 cm^2 for each sample was randomly selected for collecting the XRF signals according to the same measuring parameters (i.e., the high voltage is 50 kV, and the pixel size is 40 μm). For semi-quantitative comparisons, each XRF spectrum was normalized with the signal of Rh-Lα peak, which is generated by a Rh X-ray source.

The samples used for comparison include a black bear mandible, a bison carpal, a bison maxilla, a red deer carpal, a mammoth tooth, and a marmot mandible. Two control samples were also included: a rhinoceros mandible recovered from Jiangsu Province and a rhinoceros maxilla recovered from Guangxi Province. The two specimens were recovered from similar Pleistocene fluvial underwater sediments as that of the Harbin cranium, but the sediments belong to different drainage areas and have different depositional sources. All the mammalian fossils are housed in the Institute of Vertebrate Paleontology and Paleoanthropology, Beijing, China.

HR-ICP-MS Rare earth element (REE) analyses.

Small bone pieces (100 mg) from the nasal cavity of the Harbin cranium were carefully collected for REE and Sr isotopic analyses. For comparison, fossil fragments from seven mammals and two human individuals recovered from the Harbin area in the Songhua River were also analyzed. The age of these fossils ranges from the Middle Pleistocene to the Early Holocene (S-Fig.1,2; S-Table 1). All the fossils are deposited in the Institute of Vertebrate Paleontology and Paleoanthropology.

REE analyses were performed at the State Key Laboratory for Mineral Deposits Research, Nanjing University. The samples were processed using the method of Ref. [13]. In the laboratory, after removal of the surface contaminations using the dental drill and ultrasonically washing in the ultrapure (18.2 MΩ/cm) water, bone samples were dried and ground into powder with a mortar and pestle. The resulting powder was soaked in a pH 5 acetic acid-ammonium acetate buffer for 1 h to remove the authigenic carbonates and centrifugated and dried at 60°C overnight. About 20 mg of each sample was weighed and dissolved in 2 mL 20% HNO_3 for REE measurements. The prepared sample solutions were diluted with 2% HNO_3 by a factor of 10 before analyses. The REE concentrations were determined using a HR-ICP-MS (high resolution inductively coupled plasma mass spectrometer). The rhodium solution (10 ppb) was dropped into the sample solutions for instrument drift correction. Analytical precision was <5% for each element.

MC-ICPMS strontium (Sr) isotopic analyses

Sr isotopic analyses were performed on the fossil samples from the Harbin cranium (n=1), the Middle Pleistocene-Early Holocene mammalian fossils (S-Fig.1; S-Table 2; n=7) and human fossils (S-Fig. 2; S-Table 2; n=2) recovered from the Harbin area in the Songhua River. The sediment samples adhering to the nasal cavity of the Harbin cranium (n=1) and from a core (n=40) drilled near the Dongjiang Bridge (Fig. 1) were also analyzed. The Sr isotopic analyses were carried out at the Nanjing Normal University with a MC-ICPMS (multicollector inductively coupled plasma mass spectrometer, Thermo Fisher Neptune). Sample preparation and measure methods followed those of Ref. [14]. Samples were crushed using a mortar and pestle and cleaned

of carbonate using pH 5 acetic acid-ammonium acetate buffer. Approximately 1 mg bone powder was weighed in a 30 mL Teflon beaker and dissolved in trace-metal grade HNO_3. For sediment samples, about ~50 mg of each powdered sediment was weighed and digested using high-purity HNO_3 (1 mL) and HF (1.5 mL) for 72 h in a tightly closed Teflon vessel in an oven at 190°C. The sample solution was evaporated to dryness on a hotplate at 160°C. Dry sediment samples were repeatedly reacted with 1 mL concentrate HNO_3 to remove residual HF. All sample solutions were then evaporated to dryness, and the residues were dissolved with 0.5 mL of 3N HNO_3 at 96°C to change the medium for sample loading. The column (capacity of 1 mL) packed with 0.1 mL Sr-spec resin was used to separate Sr from other ions. The column was rinsed with 1 mL of 6N HCl and Milli-Q water to wash the residual Sr and other ions. After conditioning with 3N HNO_3, the sample solution was loaded onto the column. Sr was then eluted with 0.05 N HNO_3 and collected to evaporate to dryness. The residue was dissolved with 2% HNO_3 prior to measurements.

The samples were introduced through a nominally 50 μL min-1 capillary tube and aspirated into a Cetac Aridus II desolvating chamber running at 110°C. The Sr isotope measurement were conducted on a MC-ICPMS (Thermo Fisher Neptune). The measured $^{87}Sr/^{86}Sr$ ratio was corrected for mass fractionation by normalization to a constant $^{86}Sr/^{88}Sr$ ratio of 0.1194 using an exponential law. The isobaric interference of ^{87}Rb on ^{87}Sr was corrected using a natural $^{87}Rb/^{85}Rb$ ratio of 0.3857. Replicate measurements of the NIST SRM 987 standard yielded mean value of $^{87}Sr/^{86}Sr$ =0.710263±0.000014 (2σ, n=11) during the analytical period (S-Table 2) which is in good agreement with the data in the literature [15, 16].

The Sr isotope ratios of the Harbin cranium and mammalian/human fossils in comparions all fall into the variation range of the regional bioavailable Sr isotope ratio values in the Harbin areas (S-Fig. 3). Compared with other areas of China, the Harbin and nearby areas have the lowest bioavailable Sr isotope ratios.

MC-ICPMS Uranium-series analyses

The U-series dating samples (n = 10) were hand-drilled on the Harbin cranium with 0.3 mm carbide-tipped drill bits. To minimize destruction on the cranium, the powder sample size was kept between 0.1-0.5 mg. The locations selected for sampling all have relatively fresh bone surfaces without visible porosity. Before sampling, the bone surface was abraded to remove any superficial contamination. The powdered sample was first collected on a weighing paper, and then transferred into a clean centrifuge tube (2 ml in volume). To determine the weight of the powdered sample, the centrifuge tube was weighed before and after the sample collection with an analytical balance.

The U-series dating analyses were carried out at the Nanjing Normal University (NNU). The powdered samples were dissolved in 3N HNO_3 in a centrifuge tube, and then transferred into a Teflon beaker containing a known quantity of a ^{229}Th-^{233}U-^{236}U triple spike. One drop of $HClO_4$ was added to the sample solution to decompose organic material. The sample-spike mixture was heated overnight on a hot plate at 120°C. After the equilibration of the sample-spike mixture, U and Th were separated from each other and from other cations by passing the sample solution

through a U-TEVA resin column following the procedure of Douville et al. [17]. Firstly, the sample matrix elements were eliminated through rinsing with 3N HNO_3. Subsequently, Th was eluted using 3N HCl, and finally U was eluted using 0.5N HCl. One drop of $HClO_4$ was added to the U or Th fractions to remove any organic material derived from the U-TEVA resins. The U and Th solutions were evaporated to dryness and then dissolved in a mixture of 0.5 N HNO_3 and 0.01 N HF for U and Th isotopic analyses.

The U and Th isotopic measurements were performed on a MC-ICPMS (Thermo Fisher Neptune). It is equipped with nine Faraday cups and a secondary electron multiplier (SEM). A retarding potential quadrupole (RPQ) energy filter was positioned in front of the SEM. An Aridus-II desolvator system (Cetac) coupled with an ESI-50 nebulizer and an AutoSampler (ASX-520) were used for sample introduction. The U-Th data acquisition strategies applied here were similar to those described by Shao et al. [18]. The U isotopic data were acquired in two static sequences. The first sequence measured ^{233}U, ^{235}U, ^{236}U and ^{238}U in cups and simultaneously ^{234}U on the SEM (with RPQ-on). The second sequence shifted all masses by 1 amu to the lower mass, so that ^{233}U was measured by the SEM and the other isotopes by the cups. Thorium measurements were carried out immediately after the uranium measurements for the same sample. ^{229}Th and ^{230}Th were measured alternately on the SEM (with RPQ-on) and ^{232}Th in a cup. The U isotopes of the HU-1 standard solution were measured after every 2 samples to monitor instrumental stability.

The amplifier gains, dark noise, hydride interferences and machine abundance sensitivity were evaluated every day prior to the sample measurements. The base lines were automatically calibrated before each U isotopic measurement. Instrument memory was assessed with the SEM by introducing a blank solution before measurements of either U or Th were conducted. The relative yields of the SEM/Faraday cups were determined during U isotopic measuring by alternating the ^{233}U beam (~5 mV) on the SEM and in the Faraday cup. Instrumental mass fractionation was corrected by using an exponential function comparing the measured $^{238}U/^{235}U$ with the natural value of 137.82 for unknown samples [19]. Procedural blank was corrected by using the long-term observed values of ~0.8 fg ^{234}U, ~10 pg ^{238}U, ~0.1 fg ^{230}Th and ~2.0 pg ^{232}Th, respectively. The U-series ages (expressed here as years before 2000 A.D., b2k) were calculated by Monte-Carlo simulations[31], using half-lives of 75,584 yr for ^{230}Th[20] and 245,620 yr for ^{234}U[20], 1.4×10^{10} yr for ^{232}Th[21], and 4.47×10^{9} yr for ^{238}U[22]. All the U-series ages were corrected for the initial ^{230}Th contamination assuming an initial $^{230}Th/^{232}Th$ activity ratio of 0.8±0.4, which is a value for a material at secular equilibrium with the bulk Earth upper crustal $^{232}Th/^{238}U$ atomic ratio of ~3.8[23].

The U-series dating were also done for the mammalian/human fossils in comparison (S-Fig. 1,2; S-Table 1-3).

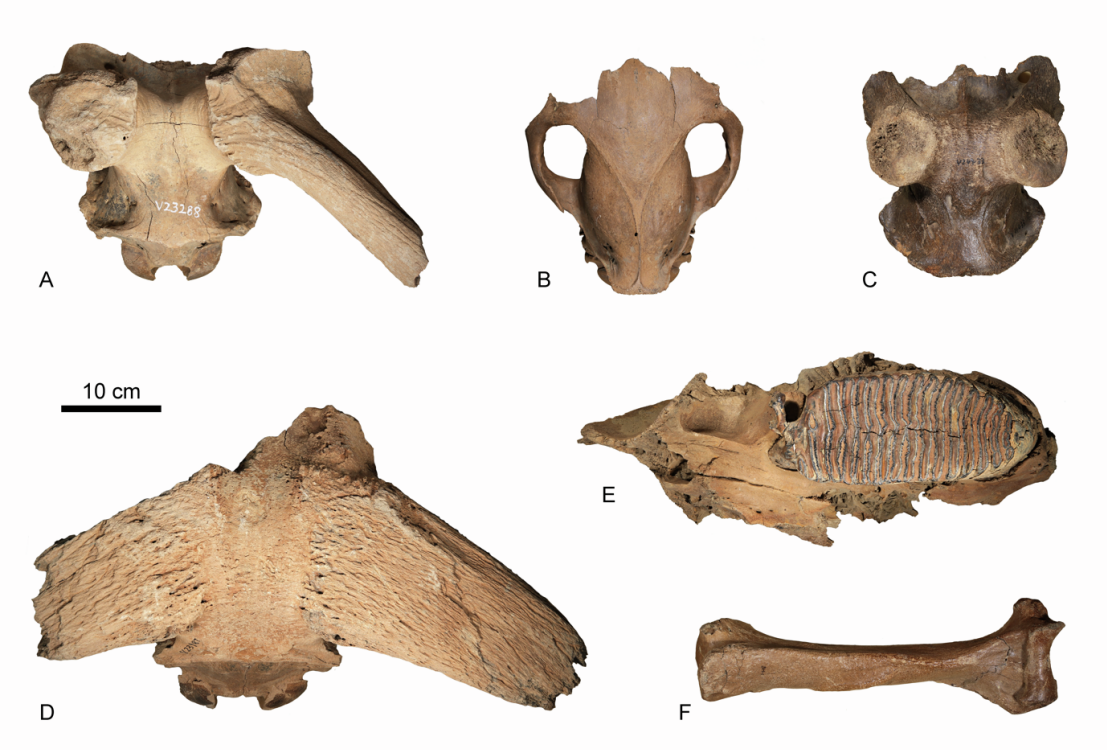

S-Figure 1. Middle-Late Pleistocene mammalian and human fossils from the Harbin area used for rare earth element concentration analyses and Sr isotopic analyses. A. V 23288, *Sinomegaceros ordosianus*. B. V 27805, *Equus przewalskii*. C. V 24433, *Cervus canadensis*. D. V 23987, *Bubalus wansjocki*. E. V 27804, *Mammuthus primigenius*. F. BH1, *Ursus arctos*.

S-Figure 2. Late Pleistocene-Early Holocene human fossils from the Harbin area used for rare earth element concentration analyses and Sr isotopic analyses. A. PA 1686. B. PA 1682.

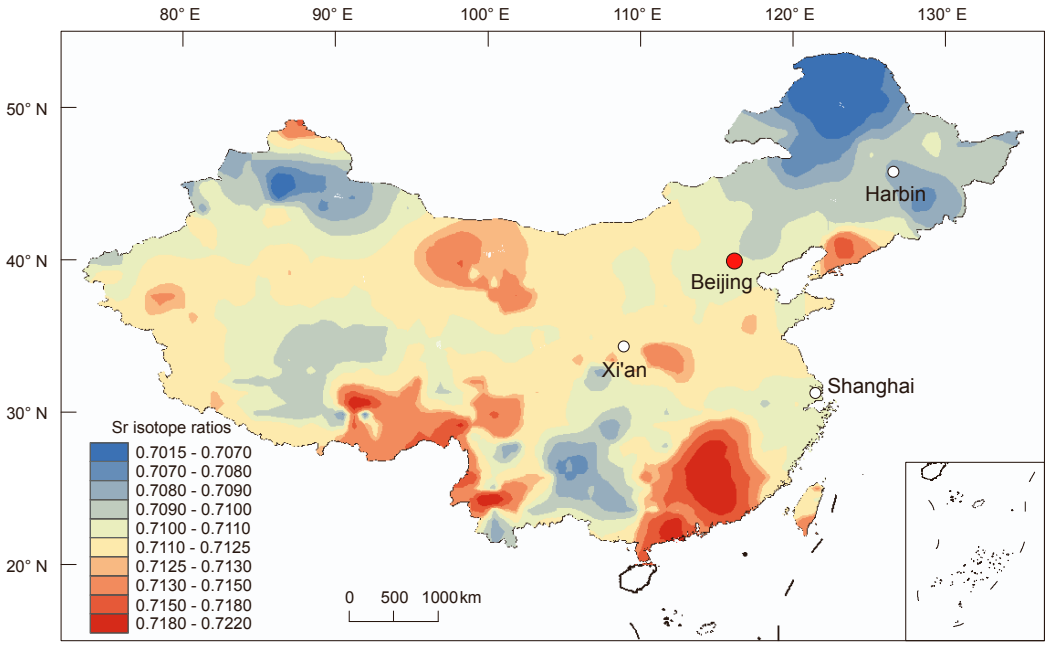

S-Figure 3. Large scale bioavailable Sr isotope map of China (data from the ref. [24], with permission).

S-Table 1. Concentrations (μg/g) of rare earth elements (REE) of the Harbin cranium in comparison with that of the Middle Pleistocene-Early Holocene human/mammalian fossils from the Harbin area

	Mammalian fossils					Human fossils			PAAS
Samples	V27805	V23987	V24433	V27804	V23288	PA1682	PA1686	Harbin cranium	
U-series Age (ka)	12±1	23.4±0.3	201±1	34.6±0.3	297±2†	9±4	17±3	148±2	
La	29.930	27.683	23.166	5.702	7.783	0.903	1.431	44.671	38.200
Ce	59.063	45.503	42.417	11.011	15.525	1.564	2.680	82.219	79.600
Pr	5.627	4.779	4.124	1.155	1.459	0.159	0.272	8.612	8.830
Nd	24.960	21.560	19.202	4.975	6.591	0.772	1.197	38.181	33.900
Sm	5.357	4.650	4.291	1.078	1.536	0.178	0.280	8.848	5.550
Eu	1.430	1.155	0.917	0.253	0.369	0.048	0.068	1.798	1.080
Gd	6.110	5.786	6.022	1.322	2.359	0.229	0.345	11.911	4.660
Tb	0.677	0.677	0.865	0.185	0.348	0.034	0.052	1.835	0.774
Dy	6.540	7.161	5.695	1.116	2.379	0.218	0.327	12.302	4.680
Ho	1.225	1.413	1.417	0.242	0.584	0.057	0.073	2.973	0.991
Er	4.398	5.371	4.491	0.703	1.819	0.176	0.222	9.383	2.850
Tm	0.527	0.671	0.636	0.100	0.259	0.025	0.031	1.361	0.405
Yb	3.056	4.069	4.047	0.617	1.586	0.171	0.192	8.951	2.820
Lu	0.545	0.755	0.709	0.099	0.270	0.032	0.032	1.536	0.433
LREE/HREE*	5.476	4.066	3.941	5.514	3.463	3.845	4.651	3.668	9.491
ΣREE**	149.445	131.233	117.997	28.557	42.867	4.566	7.203	234.580	167.160

*LREE is total content of light rare earth elements (LREE = La + Ce + Pr + Nd + Sm + Eu); HREE is total content of heavy rare earth elements (HREE = Gd + Tb + Dy + Ho + Er + Tm + Yb + Lu). **ΣREE is total content of rare earth elements (ΣREE = LREE +HREE).

† U-leaching cannot be excluded

S-Table 2. Sr isotope composition of the Harbin cranium and the adherent sediments in comparison with that of the Middle Pleistocene-Early Holocene human/mammalian fossils from the Harbin

Sample	V27805	V23987	V24433	V23288	V27804	F12	BH1	PA1686	PA1682	Harbin Cranium	Adherent sediments
U-series Ages (ka)	12.0±1	23.4±0.3	201±1	297±2†	34.6±0.3	340±3†	132.6±0.4	17±3	9±4	148±2	
$^{87}Sr/^{86}Sr$	0.709267	0.709574	0.709186	0.709137	0.709066	0.709411	0.709371	0.709165	0.709351	0.709423	0.711898
StdErr(2σ)	0.000010	0.000010	0.000010	0.000009	0.00010	0.000003	0.000004	0.000009	0.000009	0.000009	0.000003

† U-leaching cannot be excluded

S-Table 3. MC-ICPMS U-series dating results obtained on the Harbin cranium and Middle Pleistocene- Holocene mammalian and human fossils discovered in the Songhua River near the Harbin City, with uncertainties given at ±2σ level

Samples	U (μg/g)	Th (μg/g)	$^{234}U/^{238}U$	$^{230}Th/^{234}U$	$^{232}Th/^{238}U$ *	$^{230}Th/^{232}Th$	Age (ka b2k) **	Corr. $^{230}Th/^{234}U$***	Corr. Age (ka b2k) ***	$(^{234}U/^{238}U)_i$****
Harbin cranium										
HH19-1	10.28±0.02	2.929±0.008	1.548±0.005	0.474±0.003	0.0933±0.0006	7.86±0.03	66.9±0.5	0.446±0.015	62±3	1.65±0.01
HH19-2	7.64±0.02	3.042±0.008	1.566±0.007	0.593±0.004	0.1303±0.0008	7.13±0.03	91.5±0.9	0.562±0.017	85±4	1.72±0.01
HH19-3	8.99±0.02	5.96±0.01	1.503±0.004	1.039±0.004	0.2170±0.0009	7.20±0.02	305±6	1.031±0.006	296±8	2.16±0.03
HH19-4	5.191±0.003	1.174±0.002	1.481±0.002	0.798±0.002	0.0740±0.0002	15.97±0.04	151.7±0.7	0.787±0.006	148±2	1.73±0.01
HH19-5	4.850±0.004	2.462±0.003	1.519±0.003	0.973±0.003	0.1661±0.0005	8.90±0.02	241±2	0.962±0.006	233±5	2.00±0.01
HH19-6	9.958±0.005	0.629±0.001	1.503±0.002	0.653±0.001	0.0207±0.0001	47.5±0.1	106.6±0.4	0.649±0.003	106±1	1.678±0.003
HH19-7	3.971±0.003	0.669±0.001	1.508±0.003	0.950±0.002	0.0551±0.0002	25.98±0.06	225±2	0.946±0.003	223±2	1.95±0.01
HH20-1	5.212±0.002	0.922±0.005	1.543±0.001	0.984±0.001	0.0579±0.0003	26.2±0.1	248±1	0.981±0.002	245±2	2.08±0.01
HH20-2	9.729±0.004	1.097±0.006	1.508±0.001	0.738±0.001	0.0369±0.0002	30.1±0.2	130.7±0.3	0.731±0.003	129±1	1.730±0.003
HH20-3	2.562±0.001	0.666±0.003	1.576±0.001	0.891±0.001	0.0850±0.0005	16.50±0.09	188.6±0.6	0.882±0.004	185±2	1.97±0.01
Human and mammalian fossils collected from the Harbin area										
PA 1682	0.3094±0.0001	0.105±0.001	1.456±0.001	0.1339±0.0003	0.1111±0.0007	1.75±0.01	15.49±0.04	0.076±0.031	9±4	1.467±0.005
PA 1686	0.0951±0.0002	0.0325±0.0001	1.539±0.007	0.199±0.002	0.112±0.001	2.74±0.02	23.8±0.3	0.148±0.027	17±3	1.57±0.01
V 27805	5.049±0.001	0.362±0.004	1.516±0.001	0.117±0.002	0.023±0.001	7.5±0.2	13.4±0.2	0.105±0.006	12±1	1.534±0.001
V 23987	3.922±0.001	0.145±0.001	1.566±0.001	0.2010±0.0003	0.0121±0.0001	25.9±0.1	24.07±0.04	0.196±0.003	23.4±0.3	1.604±0.001
V 27804	2.286±0.001	0.0619±0.0003	1.468±0.001	0.2801±0.0005	0.0089±0.0001	46.4±0.3	35.1±0.1	0.276±0.002	34.6±0.3	1.517±0.002
BH1	9.237±0.003	0.126±0.001	1.429±0.001	0.740±0.001	0.00446±0.00004	237±2	132.8±0.4	0.739±0.001	132.6±0.4	1.624±0.002
V 24433	1.3481±0.0003	0.131±0.001	1.419±0.001	0.904±0.001	0.0317±0.0002	40.5±0.2	202.6±0.8	0.901±0.002	201±1	1.739±0.003
V 23288	0.3345±0.0001	0.0506±0.0003	1.460±0.001	1.028±0.002	0.0495±0.0003	30.3±0.2	299±2	1.026±0.002	297±2†	2.06±0.01
F12	39.413±0.007	0.143±0.001	1.205±0.001	1.011±0.001	0.00119±0.00001	1027±6	340±3	1.010±0.001	340±3†	1.536±0.004

* $^{232}Th/^{238}U$ activity ratios <0.1 indicates that the contamination of detrital ^{230}Th is insignificant for U-series age correction.

** U-series ages were calculated with half-lives of 75,584 yr for ^{230}Th (ref. [20]) and 245,620 yr for ^{234}U (ref. [20]), 1.4×10^{10} yr for ^{232}Th (ref. [21]), and 4.47×10^{9} yr for ^{238}U (ref. [22]). The ages are given at the "b2k" scale, before 2000 AD.

*** U-series ages were corrected with assumption of the initial $^{230}Th/^{232}Th$ atomic ratio of $4.4\pm2.2\times10^{-6}$, a value for a material at secular equilibrium, with the bulk earth $^{232}Th/^{238}U$ value of 3.8 and with an assumed error of 50%.

**** The back-calculated initial $^{234}U/^{238}U$ activity ratio.

† U-leaching cannot be excluded

References:

1. Bureau of Geology and Mineral Resources of Heilongjiang Province (BGMRHP), *Regional Geology of Heilongjiang Province*. People's Republic of China, Ministry of Geology and Mineral Resources, Geological Memoirs (Geological Publishing House, Beijing, 1993), vol. 33, pp. 734.
2. Wang, Y., Dong, J. and Yang, J. Quaternary Stratigraphy of the Huangshan Section in

Harbin. *Earth Science* **45**(7), 2662-2672 (2020).
3. Wei, Z., Xie, Y., Kang, C., Chi, Y., Wu, P., Wang, J., Zhang, M., Zhang, Y. and Liu, L. The Inversion of the Songhua River System in the Early Pleistocene: Implications from Sr-Nd isotopic composition in the Harbin Huangshan cores. *Acta Sedimentologica Sinica* **38**(6), 1192-1203 (2020). doi:10.14027/j.issn.1000-0550.2019.112
4. Zhan, T., Zeng, F., Xie, Y., Yang, Y., Ge, J., Ma, Y., Chi, Y., Kang, C., Jiang, X., Yu, Z., Zhang, J., Li, E. and Zhou, X. Magnetostratigraphic dating of a drill core from the Northeast Plain of China: Implications for the evolution of Songnen paleo-lake. *Chinese Science Bulletin* **64**(11), 1179-1190 (2019).
5. Institute of Vertebrate Paleontology CAS, *Pleistocene mammalian fossils from the northeastern provinces*. (Science Press, Beijing, 1959), pp. 82.
6. Zhengyi, W. The Quaternary mammalian fossils discovered in the Heilongjiang Province. , 1973, (01): 38-40. *Chinese Science Bulletin* **18**(1), 38-40 (1973).
7. Baoquan, C. and Jicai, Y. Late Pleistocene fossil mammals from Qinggang, Heilongjiang Province. *Bulletin of the Chinese Academy of Geological Sciences* **25**(131-138), (1992).
8. Huili, Y. and Wei, D. Pleistocene Mammalian fauna from the Jiaojie Cave at Acheng, Heilongjiang Province. *Quternary Science* **31**(4), 675-688 (2011).
9. Yang, Y., Li, Q., Fostowicz-Frelik, Ł. and Ni, X. Last record of *Trogontherium cuvieri* (Mammalia, Rodentia) from the late Pleistocene of China. *Quat. Int.* **513**, 30-36 (2019). doi:10.1016/j.quaint.2019.01.025
10. Ni, X., Li, Q., Stidham, T.A., Yang, Y., Ji, Q., Jin, C. and Samiullah, K. Earliest-known intentionally deformed human cranium from Asia. *Archaeological and Anthropological Sciences* **12**(4), 93 (2020). doi:10.1007/s12520-020-01045-x
11. Lu, D., Yang, Y., Li, Q. and Ni, X. A late Pleistocene fossil from Northeastern China is the first record of the dire wolf (Carnivora: *Canis dirus*) in Eurasia. *Quat. Int.*, (2020). doi:10.1016/j.quaint.2020.09.054
12. Li, J., Pei, R., Teng, F., Qiu, H., Tagle, R., Yan, Q., Wang, Q., Chu, X. and Xu, X. Micro-XRF study of the troodontid dinosaur *Jianianhualong tengi* reveals new biological and taphonomical signals. *Atomic Spectroscopy* **42**(1), 1-11 (2021).
13. Trueman, C.N., Behrensmeyer, A.K., Potts, R. and Tuross, N. High-resolution records of location and stratigraphic provenance from the rare earth element composition of fossil bones. *Geochimica et Cosmochimica Acta* **70**(17), 4343-4355 (2006). doi:10.1016/j.gca.2006.06.1556
14. Lei, H.-L., Yang, T., Jiang, S.-Y. and Pu, W. A simple two-stage column chromatographic separation scheme for strontium, lead, neodymium and hafnium isotope analyses in geological samples by thermal ionization mass spectrometry or multi-collector inductively coupled plasma mass spectrometry. *Journal of Separation Science* **42**(20), 3261-3275 (2019). doi:10.1002/jssc.201900579
15. Pin, C., Gannoun, A. and Dupont, A. Rapid, simultaneous separation of Sr, Pb, and Nd by extraction chromatography prior to isotope ratios determination by TIMS and MC-ICP-MS. *Journal of Analytical Atomic Spectrometry* **29**(10), 1858-1870 (2014).

doi:10.1039/C4JA00169A
16. Fourny, A., Weis, D. and Scoates, J.S. Comprehensive Pb-Sr-Nd-Hf isotopic, trace element, and mineralogical characterization of mafic to ultramafic rock reference materials. *Geochemistry, Geophysics, Geosystems* **17**(3), 739-773 (2016). doi:10.1002/2015GC006181
17. Douville, E., Sallé, E., Frank, N., Eisele, M., Pons-Branchu, E. and Ayrault, S. Rapid and accurate U–Th dating of ancient carbonates using inductively coupled plasma-quadrupole mass spectrometry. *Chemical Geology* **272**(1), 1-11 (2010). doi:10.1016/j.chemgeo.2010.01.007
18. Shao, Q.-F., Li, C.-H., Huang, M.-J., Liao, Z.-B., Arps, J., Huang, C.-Y., Chou, Y.-C. and Kong, X.-G. Interactive programs of MC-ICPMS data processing for ^{230}Th/U geochronology. *Quaternary Geochronology* **51**, 43-52 (2019). doi:10.1016/j.quageo.2019.01.004
19. Hiess, J., Condon, D.J., McLean, N. and Noble, S.R. ^{238}U/^{235}U Systematics in Terrestrial Uranium-Bearing Minerals. *Science* **335**(6076), 1610-1614 (2012).
20. Cheng, H., Lawrence Edwards, R., Shen, C.-C., Polyak, V.J., Asmerom, Y., Woodhead, J., Hellstrom, J., Wang, Y., Kong, X., Spötl, C., Wang, X. and Calvin Alexander, E. Improvements in ^{230}Th dating, ^{230}Th and ^{234}U half-life values, and U–Th isotopic measurements by multi-collector inductively coupled plasma mass spectrometry. *Earth and Planetary Science Letters* **371-372**, 82-91 (2013). doi:10.1016/j.epsl.2013.04.006
21. Holden, N.E. Total half-lives for selected nuclides. *Pure and Applied Chemistry* **65**(5), 941-958 (1990). doi:10.1351/pac199062050941
22. Goldstein, S.J., Murrell, M.T. and Janecky, D.R. Th and U isotopic systematics of basalts from the Juan de Fuca and Gorda Ridges by mass spectrometry. *Earth and Planetary Science Letters* **96**(1), 134-146 (1989). doi:10.1016/0012-821X(89)90128-3
23. Hans Wedepohl, K. The composition of the continental crust. *Geochimica et Cosmochimica Acta* **59**(7), 1217-1232 (1995). doi:10.1016/0016-7037(95)00038-2
24. Wang, X. and Tang, Z. The first large-scale bioavailable Sr isotope map of China and its implication for provenance studies. *Earth-Science Reviews* **210**, 103353 (2020). doi:10.1016/j.earscirev.2020.103353